JOURNAL OF AIRCRAFT
Vol. 39, No. 3, May–June 2002

Quantitative Comparison of Ice Accretion Shapes on Airfoils

Gary A. Ruff*
Drexel University, Philadelphia, Pennsylvania 19104

The need to compare quantitatively ice accretions that form on aircraft during flight in icing conditions has recently expanded from a research-oriented activity to more general applications. For example, verification of the calibration of ground-test facilities is often performed by comparing ice shapes produced at a specific icing condition. Because icing tests in ground facilities are important in the aircraft certification process, concerns about the subjectivity and consistency of these ice shape comparisons have increased. The ice accretion comparison method presented uses geometric features as well as several parameters extracted from a *P*-Fourier descriptor of the ice accretion profile to develop a single parameter that can be used to rank how well two ice shapes compare. The results of this automated method were found to be consistent with comparisons of ice accretions made visually and based on percent differences of geometric characteristics. Also, for comparisons of ice shapes having a calculated comparison parameter less than 0.075 (7.5%), the drag coefficient of the iced airfoils differs by less than 10%. Higher values of the comparison parameter produce greater visual differences in the ice accretions and larger variations in the drag coefficient.

Nomenclature

a_k	=	Fourier descriptor (coefficients of the Fourier transform)
c	=	airfoil chord, cm
c_d	=	drag coefficient (two-dimensional)
c_l	=	lift coefficient (two-dimensional)
f	=	frequency, cycles/(s/c)
s	=	surface distance, cm
w	=	normalized line segment array
x, y	=	airfoil coordinates, cm
x_i	=	measurement of geometric characteristic i
z	=	complex line segment array
$\overline{\Delta c_d}$	=	normalized difference in drag coefficients, Eq. (11)
δ	=	uniform line segment length, s/c

Introduction

THE comparison of the ice accretions that form on aircraft surfaces and the effect these accretions have on aerodynamic performance plays an integral part in aircraft icing research and flight certification. The need to compare quantitatively ice accretion shapes has recently expanded from being a research-oriented activity, such as for the development of icing scaling techniques or the evaluation of numerical simulations, to more general applications. Some of these applications, such as the verification of ground-test simulation capability and the comparison of calibrations between test facilities, frequently have important implications regarding aircraft certification. It is, therefore, critical that these comparisons of ice accretion shapes be made as consistently and quantitatively as possible. However, the range of objectives of the applications that require two ice accretions to be compared places significant demands on any proposed technique. A practical method to compare ice accretions should be 1) easy to apply at different icing facilities, 2) applicable to glaze, rime, and mixed icing conditions, 3) applicable to the comparison of experimentally and numerically produced ice accretions, 4) independent of test article geometry, and 5) free from the subjectivity of the operator.

Received 8 October 1999; revision received 18 February 2001; accepted for publication 19 February 2001.

*Associate Professor, Department of Mechanical Engineering and Mechanics; currently Aerospace Engineer, Microgravity Combustion Science Branch, NASA John H. Glenn Research Center at Lewis Field, MS 77-5, 21000 Brookpark Road, Cleveland, OH 44135. Associate Fellow AIAA.

The first step in comparing ice accretions is to determine which characteristics should be compared. Generally either geometric characteristics of the ice accretion or aerodynamic performance parameters are proposed for comparing accretions.[1–4] These parameters should be evaluated based on their ability to satisfy the five requirements just listed. Although the ultimate objective of many icing tests is to determine the aerodynamic performance of a test article with accreted ice, the measurement of lift, drag, and moment coefficients in an icing wind tunnel introduces another level of complexity and uncertainty into the test procedure. Not all icing test facilities are equipped to measure aerodynamic coefficients that would limit the usefulness of these parameters in a standardized comparison method. In icing test facilities that are equipped to make aerodynamic measurements, turbulence levels are generally higher than in true aerodynamic test facilities and can significantly affect the measurement. The use of aerodynamic parameters to compare experimentally and numerically produced ice accretions is also problematic because the determination of accurate performance parameters from a numerical simulation of the icing process is an area of active research.[5] For these reasons, recent applications of ice accretion comparison methodologies have focused on the comparison of specific geometric features.[1,2] However, because the aerodynamic performance is so critical to the comparison of aircraft ice accretions, an additional constraint on a practical comparison method is that ice shapes determined to compare well should also have similar aerodynamic performance parameters.

The use of geometric characteristics of ice accretions as comparison parameters satisfies many of the constraints listed earlier. Measurements can be made at any icing test facility and are applicable to both experimental and numerical ice accretions. Several ice accretion comparison methods that make use of various geometric parameters have been reported. Ruff and Anderson[1] have used six geometric parameters to characterize an ice accretion shape. These parameters, illustrated in Fig. 1, are the thickness of the ice accretion at the stagnation point, maximum thickness, maximum width of the ice accretion, impingement width, horn length, and horn angle. These parameters were measured from a digitized image using CAD software and comparisons made by calculating the percent difference in each of the measurements between the two accretions. The percent differences for all of the pairs of measurements were then averaged to serve as a measure of the merit of the comparison of the ice shapes. This method was found to agree very well with a subjective ranking of the similarity between pairs of ice accretions. Ruff and Anderson[1] also applied a fuzzy inference system to aid in the interpretation of these data, although the results were similar to those obtained by comparing the average percent

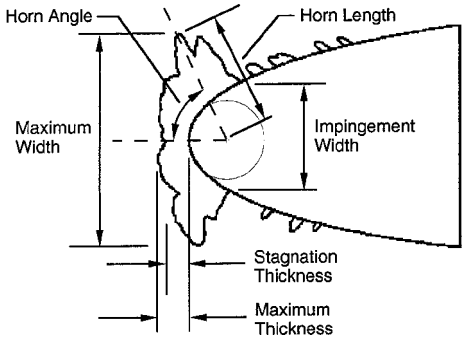

Fig. 1 Geometric characteristics of ice accretion used in quantitative analysis of Ruff and Anderson.[1]

difference of the measured quantities. Wright and Rutkowski[2] developed an automated method to determine 11 geometric characteristics of an ice accretion from digitized coordinates. In this method, the characteristics are extracted from a plot of the ice thickness as a function of surface distance and include 1) upper and lower icing limits, 2) upper and lower surface maximum thickness, 3) minimum thickness between these two maximums, 4) upper and lower surface angle at maximum thickness, 5) upper and lower surface ice area, 6) total ice area, and 7) total included angle between upper and lower maximum thickness.

The data set described in Ref. 2 includes experimental and predicted ice accretions for 231 icing conditions. For these 231 conditions, there is a database of 842 experimental ice shapes from repeat conditions and off-centerline locations. When repeat experimental ice shapes were available, an experimental average for each of the features listed was calculated, and measurements from predicted and experimental ice shapes were compared to these average dimensions. Various averages of these percent differences were formed and used to draw conclusions about the overall comparison of predicted and experimental ice accretions. A single comparison parameter to rank the quality of the comparison of two ice shapes was formed from these averages, but the performance of this parameter relative to a visual comparison of the ice shapes or aerodynamic performance was not evaluated. Subsequently, Wright and Chung[3] have calculated performance coefficients for ten experimental ice shapes and the associated LEWICE[6] predictions from those icing conditions. A regression analysis was performed to determine which of the 11 ice shape parameters defined in Ref. 3 and listed here correlated best with the lift, drag, and moment coefficients. The results of this work will be discussed in detail later in this paper.

If geometric features are to be used to compare ice accretions and should be related to aerodynamic performance, it is logical to examine previous studies that have investigated the effect of ice geometric features on changes in aerodynamic coefficients. In 1958, Gray correlated the geometric measurements of upper surface horn length and horn angle from an ice accretion with the impingement rates, icing conditions, and drag coefficients.[7] Subsequently, he expanded this correlation of ice accretion geometry with icing conditions to additional airfoils. Gray used this larger database to develop a correlation to predict the aerodynamic penalties caused by ice accretion on various airfoils as a function of the impingement rates and icing conditions.[8] This was a very unique and potentially useful correlation, although later work indicated that the increase in drag coefficient caused by the ice accretion was frequently overpredicted.[9,10] Papadakis et al.[11] conducted an experimental evaluation to determine the effects of leading-edge ice accretion geometry on airfoil performance. In these tests, they measured the lift, drag, pitching moment, and pressure coefficients for a NACA 0011 airfoil, on which spoilers had been placed to simulate the ice accretion. Tests were run using 61-cm- and 30.5-cm-chord airfoils with spoiler heights of 3.8 and 7.6 cm. These heights were selected to correspond to 22.5- and 45-min glaze ice accretions that had been formed on this airfoil during icing tests. The spoilers were placed at angular locations around the leading edge of the airfoil, simulating the location of the horn of an ice accretion. Parametric studies of horn height, horn angle, and horn location were conducted for three Reynolds numbers. They found that the height of the structure and its location on the surface played an important role in performance degradation, with the simulated ice structures having the largest height, reducing $c_{l\,\max}$ by up to 76% and increasing c_d by up to 13 times that of the clean airfoil. Lee et al.[12] reported similar study in which they also attached simulated ice structures to the leading edge of a natural laminar flow airfoil (NLF-0414F). These structures had heights of $0.067c$, $0.0433c$, and $0.02c$ and were placed at one of six s/c locations around the leading edge of the airfoil ($s/c = 0.034$, 0.017, 0.0085, 0.00, -0.075, and -0.015). They too found that the height of the structure and its location on the surface played an important role in performance degradation, with the simulated ice structures having the largest height producing the greatest effects on c_l and c_d. The height and location of the simulated ice structures used by Papadakis et al.[11] and Lee et al.[12] roughly correspond to the horn length and angle used by Gray[7,8] to correlate drag coefficients.

Even though aerodynamic performance of iced airfoils has been investigated using horn length and horn angle, these two geometric characteristics alone are not sufficient to form a satisfactory comparison method. For example, whereas glaze ice typically has an upper and lower horn on both sides of a stagnation point, only the upper horn was used by Gray[7,8] to correlate aerodynamic performance. However, the size and shape of the lower horn affects the appearance of an ice accretion and does play a role in determining the drag coefficient.[10] Gray[7,8] considered a rime ice accretion as a single horn that formed on the leading edge of an airfoil. Therefore, any comparison method that would make use of both an upper and lower horn would not be directly applicable to rime ice accretions. Icing conditions that produce accretions having both rime and glaze portions frequently have glaze horns near the leading edge and large rime feathers further aft. Although there are glaze horns on these accretions, the rime portions can have an effect on the flow and, therefore, on the performance of the iced airfoil. Obviously, glaze, rime, and mixed ice accretions have different geometric features that make the selection of a single set of relevant parameters difficult. Increasing the number of features measured to ensure all situations are addressed is also problematic. If several features to be measured are redundant or missing from a particular ice shape, the interpretation of a single average comparison parameter can be ambiguous. Ideally, an ice accretion comparison method will contain as few parameters as possible while ensuring that the most significant features of the ice accretion are represented.

Objective

The objective of this paper is to develop a method to quantify the geometric characteristics of an ice accretion and to use these characteristics to compare two ice accretions. The output from this method is a comparison parameter that ranks the quality of the comparison. This paper begins with a description and justification of the methods to be used to geometrically compare ice shapes, followed by a presentation of the experimental methods used to obtain the ice accretions. The performance of the automated method is evaluated by comparing it with average percent differences of a set of measured geometric characteristics. The difference in the aerodynamic performance of compared accretions is also evaluated in terms of the comparison parameters.

Two-Dimensional Pattern Recognition

The automatic quantification of ice accretion characteristics has many similarities with two-dimensional pattern recognition. The comparison of geometric characteristics of ice accretions is an example of a feature-based pattern recognition method that makes use of geometrical or topographical features (local features). Feature-based methods can also make use of global features that are extracted from a transformation algorithm. Methods applying Fourier (see Refs. 13–16), Hough (see Ref. 17), Walsh (see Refs. 18 and 19), and wavelet[20] transformations of a two-dimensional profile have been developed. The use of local geometric features is conceptually simple and can clearly describe relevant features. However, it can be difficult to extract the required measurements, and these methods generally require more user intervention to help interpret features.[21]

Transform methods are more robust in that they require less user intervention to extract the variables used in the comparison. However, their ability to describe specific features is not as straightforward as that of geometric methods. Hybrid feature-based methods that make use of both global and local parameters have been relatively successful in handling difficult pattern recognition tasks such as automatically identifying hand-written characters.[22,23] One important difference between pattern recognition methods and a method to compare ice accretions is that the objective in most pattern recognition applications is to determine if an unknown geometry matches one of the geometries stored in a database. An ice accretion comparison method must not only be able to determine if two geometries are the same, but must also consistently quantify any differences between them. Thus, two-dimensional pattern recognition schemes may serve as a starting point for the development of a comparison method, but one or more comparison parameters will have to be identified and evaluated.

Description of the Ice Accretion Comparison Technique

In this section, the details of the hybrid comparison method will be presented. As discussed earlier, the ice accretion comparison method resulting from this work uses parameters derived from both structural and transform methods. First, the transform technique used to characterize the global features will be discussed and several examples presented to illustrate the physical significance of the descriptors. The technique used to compare ice accretions and quantify the differences between them will then be described.

P-Fourier Transform Methodology

The use of Fourier descriptors was first introduced by Cosgriff[13] in 1960. In general, a starting point on a boundary curve is selected, and a function is defined that measures the slope of the curve as a function of arc length. This function is normalized and expanded in a Fourier series. The set of Fourier coefficients comprises the shape features to be analyzed and the coefficients form the Fourier descriptors of the original curve. Early work in this method of pattern recognition indicated that "look-alike shapes are usually near each other in a space of Fourier descriptor features. . . ."[14] Uesaka[15] presented a Fourier descriptor that is applicable to open and closed curves and named it the *P*-Fourier descriptor. Because these descriptors are based on the slopes of segments of a curve, the technique is invariant under the parallel translation and enlargement/reduction of the curve being evaluated. This method has recently been applied to the automatic recognition of human face profiles,[16] a problem very similar in concept to the comparison of ice accretions. The current approach is to calculate the *P*-Fourier descriptor for the two-dimensional profile of an ice accretion shape and develop appropriate metrics to compare the shapes using this descriptor. In the following paragraph, the *P*-Fourier transform method applied in this work is described. The terminology follows that given in Ref. 16.

Let the curve defining the perimeter of the ice accretion be represented by line segments on a two-dimensional complex plane

$$z(j) = (x/c)(j) + i(y/c)(j), \qquad j = 0, 1 \ldots, n \tag{1}$$

where x and y are the digitized airfoil coordinates, c is the airfoil chord, and $i = \sqrt{(-1)}$. Let the length of each line segment comprising the profile curve be constant and equal to δ. Then, from Eq. (1),

$$\delta = |z(j+1) - z(j)|, \qquad j = 0, 1, \ldots, n-1 \tag{2}$$

Each line segment can then be normalized by δ to form line segment array $w(j)$. From Eqs. (1) and (2), this is

$$w(j) = [z(j+1) - z(j)]/\delta \tag{3}$$

The discrete Fourier expansion of $w(j)$ becomes

$$w(j) = \sum_{k=0}^{n-1} a_k \exp\left(2\pi i \frac{jk}{n}\right) \tag{4}$$

where the Fourier coefficients a_k, $k = 0, 1, 2, \ldots$, are

$$a_k = \frac{1}{n} \sum_{j=0}^{n-1} w(j) \exp\left(-2\pi i \frac{jk}{n}\right) \tag{5}$$

The set of a_k is the *P*-Fourier descriptor. The spatial frequency associated with the a_k is given by

$$f_k = [k/(n-1)](f_s/2), \qquad k = 0, 1, \ldots, n-1 \tag{6}$$

where f_s is the sampling frequency given as $1/\delta$. The units on δ are surface length/chord (s/c) making the units of f_k = cycles per nondimensional surface length, that is, cycles/(s/c).

Geometric Significance of the Fourier Coefficients

One of the shortcomings of transform methods of pattern recognition is that it is more difficult to describe specific features of a profile than it is when using structural methods. However, the features are represented by the Fourier descriptors, and information about them can be extracted. In this section, the geometric significance of the Fourier coefficients is examined.

Simulated ice accretion. A sinusoidal function having the form

$$x = -\{2 \sin[2\pi y(0.5)] + A \sin[2\pi y(B)]\} \tag{7}$$

was constructed to illustrate the behavior of the *P*-Fourier descriptor. As shown in Fig. 2, when $A = 0$ and this function is plotted from $y = 0$ to 1, the profile resembles the leading edge of an airfoil. For nonzero values of A and B, sinusoidal roughness elements are superimposed onto the airfoil shape with the value of A determining the height of the elements. The frequency of the roughness is specified by B. The profiles for $B = 10$ and $A = 0.1$ and 0.3 are shown in Fig. 2. Figure 3 shows the magnitude of the Fourier coefficients for these two cases as a function of frequency. For both values of A, the first frequency peak is located at $f = 1$ cycles/s, that is, cycles/unit surface distance, because of the limited resolution of the discrete Fourier transform. The second frequency peak occurs at $f = 10$ cycles/s, which corresponds to the frequency of the superimposed waveform. The peaks at higher frequencies are harmonics of the function up to approximately $f = 50$ cycles/s, where the frequency components are primarily discretization noise. When the magnitude of the coefficients at $f = 10$ cycles/s are compared, it is observed that the waveform produced with the larger roughness elements ($A = 0.3$) produced a significantly greater coefficient than that with $A = 0.1$. Based on these results, it is observed that the frequency content of a two-dimensional profile can be quantified from the Fourier descriptor for that profile. The magnitude of the coefficients is also an indication of the size of the geometric features on the two-dimensional profile.

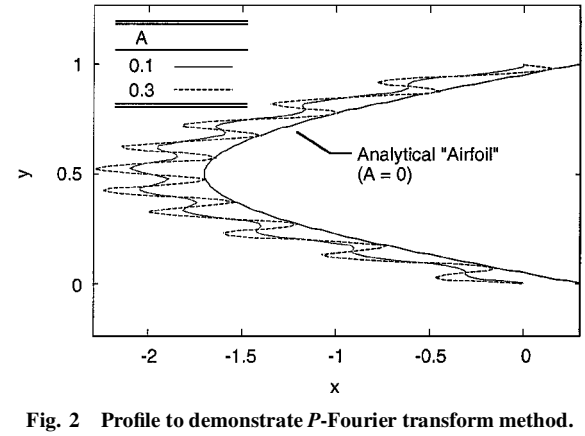

Fig. 2 Profile to demonstrate *P*-Fourier transform method.

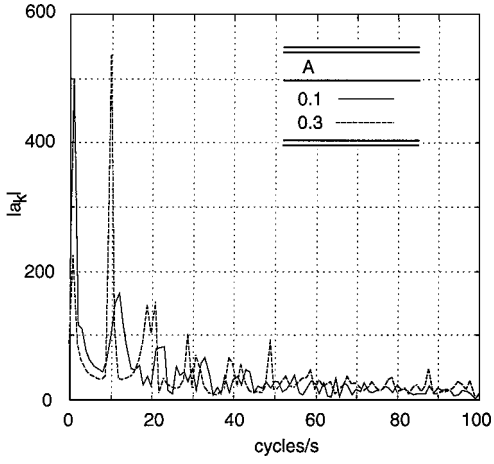

Fig. 3 Fourier descriptor of analytic profile.

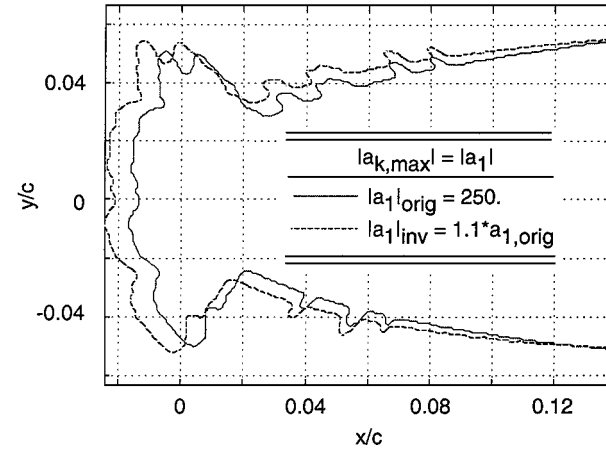

Fig. 5 Effect of magnitude of maximum coefficient on ice accretion profile.

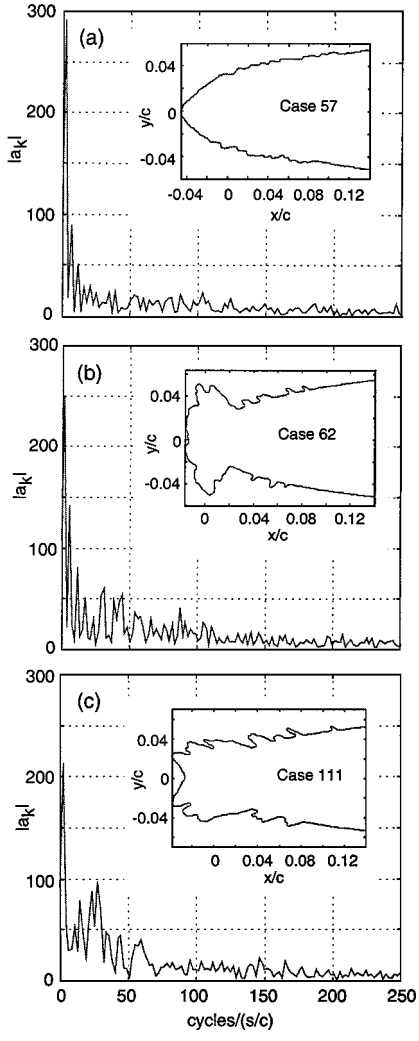

Fig. 4 Fourier descriptors and associated ice shapes for a) rime, b) glaze, and c) mixed ice accretions.[24]

Type of ice. Unlike the preceding example, the shape of an ice accretion is not described by a single frequency, but by a range a frequencies. Because glaze, rime, and mixed ice accretions have different geometric characteristics, these differences should be evidenced in the Fourier descriptors. The algorithm described in the preceding section was applied to representative rime, glaze, and mixed ice accretion shapes and the results are shown in Fig. 4. The inset in each sub-figure of Fig. 4 shows the associated ice accretion profile and run identification number used by Anderson and Ruff.[24] In Fig. 4a, the magnitude of the coefficients of the rime ice accretion decreases very quickly. The maximum coefficient is in the second frequency bin, similar to the simulated accretion shown in Fig. 3. The glaze ice accretion shown in Fig. 4b has its maximum peak in the second frequency bin, but has a significantly broader frequency spectrum, extending out to approximately 100 cycles/(s/c). The magnitude of the Fourier coefficients of the mixed ice accretion shown in Fig. 4c extends to frequencies of about 60–100 cycles/(s/c), between those for the rime and glaze accretions. As shown in Fig. 4, rime, glaze, and mixed ice accretions can be differentiated by their Fourier descriptors with glaze ice accretions having the broadest frequency content.

Magnitude of the coefficients. We can also investigate how the magnitude of Fourier coefficients represents an ice accretion geometry by calculating the Fourier coefficients, modifying the value of one or more of the coefficients, and performing an inverse Fourier transform to reconstruct the x and y coordinates from the modified coefficients. The effect of the modification can be evaluated by comparing the modified profile with the original. For example, Fig. 5 shows the original ice accretion profile and a profile generated after increasing the value of the maximum Fourier coefficient by 10%. (A glaze ice accretion was used for this investigation because glaze ice was found to have a broader frequency content than rime or mixed ice shapes.) Note that the right-hand portion of the shape was not changed, but that the rest of the tracing was stretched to the left. Therefore, all other coefficients being equal, the magnitude of the maximum coefficient is seen to be a measure of the size of the ice accretion. Similarly, modifying higher coefficients was found to have a decreasing effect on the ice accretion shape.

Number of coefficients. The next question to be addressed is how many coefficients are required to describe accurately an ice accretion? To answer this question, the coefficients of the Fourier descriptor were calculated, a portion of them were set to zero, and the inverse transform operation was performed. The reconstructed ice accretion was then compared to the original profile. Figure 6 shows the results when all frequencies greater than 25, 50, and 100 cycles/(s/c) were set equal to zero. Although the general shape of the ice accretion is captured by frequencies lower than 25 cycles/(s/c), frequencies out to at least 100 cycles/(s/c) must be included before there is no significant difference between the original and inverse profiles. Note that the general location of the horns of the glaze accretion is captured by the lowest frequency components. As an aside, this technique appears to be an excellent method of obtaining the coordinates for smoothed ice accretions used in various types of icing testing.

Based on these investigations, it was concluded that the frequency content of the ice accretion profile does depend on the type of ice accretion, with glaze ice having the largest Fourier coefficients at

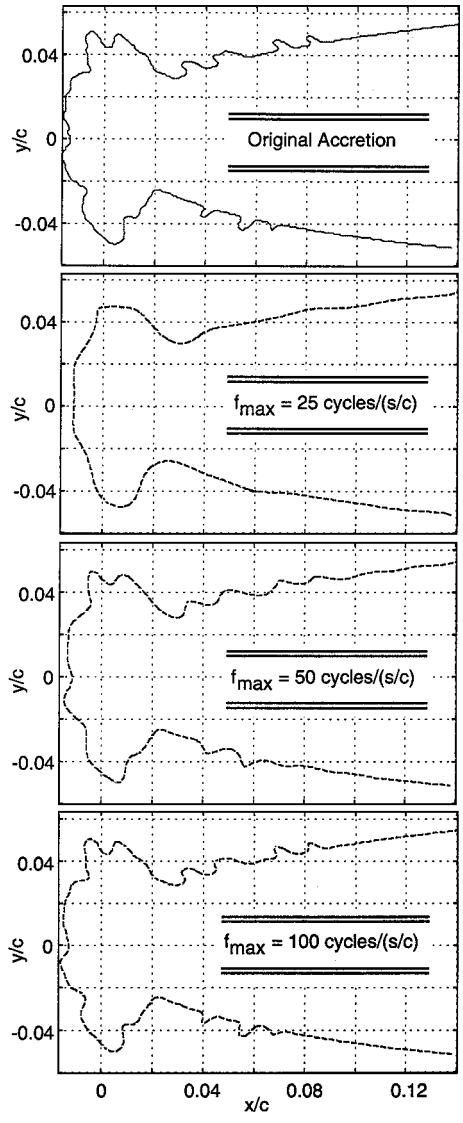

Fig. 6 Evaluation of frequencies required to reconstruct ice accretion profile.

higher frequencies. The magnitude of the maximum coefficient represents the size of the ice accretion. Frequencies out to approximately $f = 100$ cycles/(s/c) are required to accurately describe a typical ice accretion shape to the resolution available by the ice tracing technique.

Difference Terms

The preceding discussion showed that the coefficients of the Fourier descriptor are directly related to the geometry of the ice accretion profile. However, to compare ice accretion shapes, it is necessary to develop parameters that quantify the differences between two sets of Fourier descriptors. Because the magnitude of the maximum coefficient was found to be representative of the size of the ice accretion, the normalized difference in the magnitude of the maximum coefficient was selected as a comparison parameter. This can be expressed as

$$E_1 = \frac{|a_{\max,2} - a_{\max,1}|}{\frac{1}{2}[a_{\max,2} + a_{\max,1}]} \tag{8}$$

The subscripts 1 and 2 denote a parameter from one of the two ice accretions being compared. Note that the absolute value of the numerator is specified. As shown in Fig. 4, the frequency content is representative of the type of ice as well as the presence and location of horns. Therefore, a second difference term was formed by summing

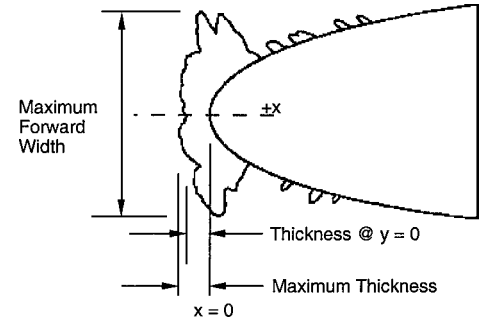

Fig. 7 Geometric parameters used in hybrid comparison method.

the frequency-weighted, normalized difference in the Fourier coefficients from $f = 0$ to 100 cycles/(s/c). This is expressed as

$$E_2 = \sum_{k=1}^{K} \frac{1}{f_k} \frac{|a_{fk,2} - a_{fk,1}|}{\frac{1}{2}[a_{fk,2} + a_{fk,1}]} \tag{9}$$

A frequency weighted difference parameter was applied because the coefficients at higher frequencies were found to have significantly less influence on the ice accretion profile.

Measurement of Geometric Parameters

As discussed earlier, many practical two-dimensional pattern recognition schemes make use of both global and local parameters to make use of the strengths of both of these methodologies.[22,23] Accordingly, the comparison method developed in this work used not only difference parameters from the P-Fourier descriptor described, but also several geometric parameters that could be easily extracted from the digitized ice accretion profile. Specifically, the geometric parameters are the maximum forward width, maximum thickness, and the ice thickness at $y = 0$ and are illustrated in Fig. 7. The maximum thickness and ice thickness at $y = 0$ are measured from the vertical axis at $x = 0$. The maximum forward width is the maximum width of the ice accretion upstream of the leading edge. Note that these features define a region in which the ice accretion is located. The fractional difference in these measurements was calculated using the equation

$$\Delta x_i = \frac{|x_{i,2} - x_{i,1}|}{\frac{1}{2}[x_{i,2} + x_{i,1}]} \tag{10}$$

where x_i is the value of the ith geometric characteristic.

The first step in the comparison process was to digitize a two-dimensional tracing of each ice accretion profile. The P-Fourier descriptors for pairs of ice accretions was calculated using the x and y coordinates obtained as a result of the digitization. The difference parameters given by Eqs. (8) and (9) were then calculated, and the geometric parameters identified in Fig. 7 were measured. The average of the five difference parameters from this technique (maximum forward width, maximum thickness, thickness at $y = 0$, normalized difference in maximum coefficient, and the sum of the frequency-weighted normalized difference in the coefficients) was calculated to obtain a single parameter to characterize the comparison. The entire process, including digitization, analysis, and comparison, was automated in a MATLAB®[25] program.

Experimental Methods

Tests to investigate the selection of the model velocity in icing scaling methods were performed in the NASA John H. Glenn Research Center at Lewis Field Icing Research Tunnel (IRT) in March and May of 1998.[24] The IRT is a closed-loop tunnel with a refrigeration system that permits control of temperature from −30 to 4°C. A water-spray system provides a range of liquid-water content and water droplet size that covers a significant portion of the Federal Aviation Administration Part 25 Appendix C icing envelope. The test section has dimensions of 1.8 by 2.7 m, and velocities of up to 160 m/s are possible. Tests were performed using two-dimensional

NACA 0012 airfoils with chords of 53.3, 35.6, and 26.7 cm mounted vertically across the 1.8-m span of the IRT test section. All of the solid aluminum models had a span of 61 cm and were placed between end plates to reduce end effects. The models had a uniform chord and were unswept. A set of test conditions were selected to represent reference cases, and the various scaling methods were applied to determine the corresponding scale test conditions. Tests were run at both sets of conditions: Two-dimensional cuts through the resulting ice accretions were made at the center of the tunnel test section and 20.3 cm above the centerline, and ice shapes were recorded by tracing the ice outline onto a cardboard template.

Previous work has shown that an average difference parameter calculated from measurements of a set of six geometric parameters yields essentially the same ranking of the quality of a comparison as that done by observation.[1] The geometric parameters included in this set were illustrated in Fig. 1. To compare experimental ice accretions, 21 pairs of conditions visually judged to represent good, fair, and poor comparisons were selected from the data set of ice accretions obtained during the icing scaling tests conducted in 1998.[24] The 10 pairs of ice accretions presented in Ref. 3 were used to evaluate the ability of the method to compare experimental and computational ice accretion shapes. For each pair of ice accretions, the geometric characteristics were measured, and the nondimensional fractional difference of each characteristic was calculated using Eq. (10). The average of the Δx_i, that is, $\overline{\Delta x}$, was also calculated to yield a single measure of the comparison using this geometric method. The comparisons in this data set had values of $\overline{\Delta x}$ that ranged from 0.020 to 0.412. The hybrid ice accretion comparison method should yield results that agree with the visual and geometric-based rating of how well two ice accretions compare. This will be discussed in the following section.

Comparison of Ice Accretion Shapes

Figure 8 shows four pairs of experimental ice accretions that represent a range of quality of shape comparisons. The values of the geometric and hybrid comparison parameters are shown in each subfigure of Fig. 8. The value of these parameters are not equal, but both rate the quality of the comparison fairly well, with the lower values indicating the better comparison. Note that the ranking of the quality of the comparisons is different depending on which parameter is used. For example, the hybrid method ranks the comparisons in the order of Figs. 8a–8d with Fig. 8a being the best comparison. The geometric method ranks them Figs. 8a, 8d, 8b, and 8c. The difference occurs because the Fourier descriptor method identifies the difference in the rime feathers along the upper and lower surface of Fig. 8d that is missed in the geometric method. The hybrid method is observed to be at least as effective in ranking the quality of the comparisons as the average fractional difference of the geometric parameters.

Figure 9 shows comparisons experimentally produced (solid line) and computationally produced (broken line) ice accretions from Ref. 3. Note that the hybrid comparison parameter for Figs. 9a–9c, differ by less than 0.05, indicating that the quality of the comparisons are similar. Visually, the comparisons shown in these three subfigures of Fig. 9 are of approximately equal quality. The comparison of the geometric parameters indicates that the comparisons shown in Figs. 9a and 9c are considerably better than that in Fig. 9b. The comparison in Fig. 9d is the worst for both the geometric and hybrid comparison parameters because of the obvious large differences between the two accretions.

Figure 10 shows the average difference parameter for all 31 cases, plotted as a function of the average fractional difference of the geometric measurements. As was shown in Figs. 8 and 9, the values of the hybrid and geometric comparison parameters are not equal, but the hybrid comparison parameter is shown to correlate fairly well with the average of the geometric features. The differences between these parameters occur because the P-Fourier transform methodology is sensitive to the frequency content of the overall ice accretion profiles, not to a difference in any particular feature. This is clearly demonstrated in Fig. 11, which compares the frequency content of experimentally and computationally produced ice accretions. (The two ice shape profiles are overlaid in the inset of Fig. 11.) At the

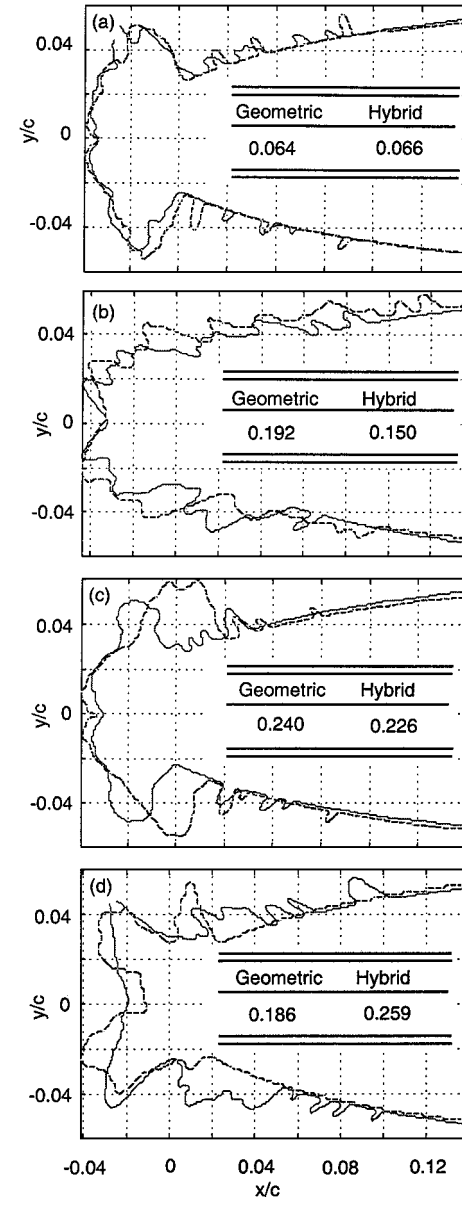

Fig. 8 Comparison of experimental ice accretion shapes and associated geometric and hybrid comparison parameters.

lowest frequencies, the Fourier coefficients compare very well, indicating that the general shape of the accretions is similar. However, the magnitude of peaks at approximately 10 and 14 cycles/(s/c) in the Fourier descriptor for the computed ice accretion are larger because the glaze horn on the upper surface of the computed accretion is larger than that on the experimental ice accretion. Starting at about 20 cycles/(s/c), the magnitude of the Fourier coefficients decays more rapidly for the computed ice accretion. This is because the mechanisms that produce the roughness elements on the surface of an ice accretion and contribute to the higher-frequency components are not modeled in LEWICE.[6] However, because the shape of the ice accretion is primarily determined by the coefficients at lower frequencies, the absence of the high-frequency components does not generally degrade the visual comparison. The value of the hybrid comparison parameter for these two cases is 0.158 that, based on the comparisons shown in Figs. 8 and 9, is consistent with the visual comparison of the ice shapes.

Comparison of Aerodynamic Performance

It is also important that two ice accretions that are judged to be geometrically similar using a comparison method are also aerodynamically similar. Olsen et al.[10] measured the drag coefficients

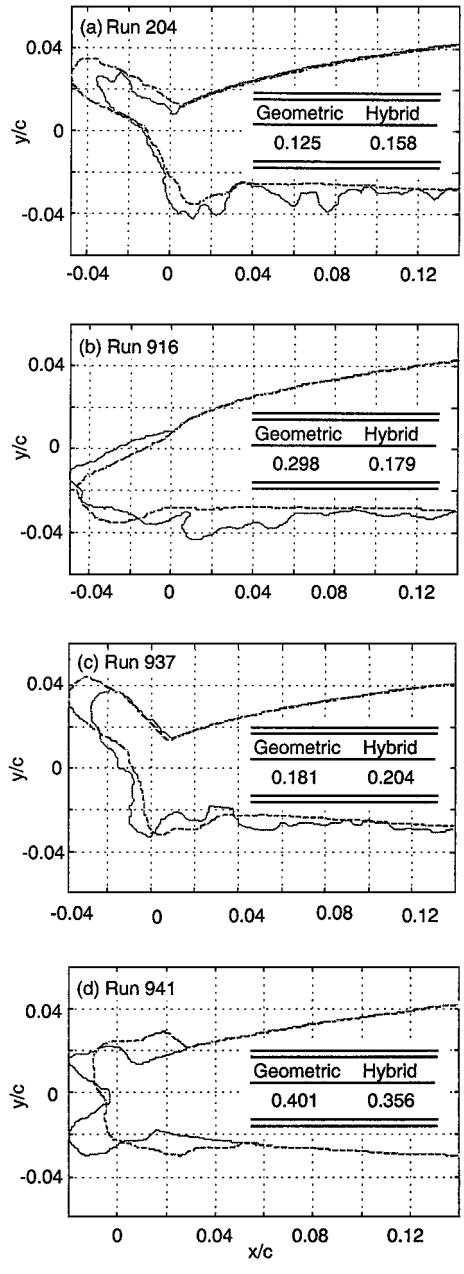

Fig. 9 Comparison of experimental (solid line) and computational (dashed line) ice accretion shapes and associated geometric and hybrid comparison parameters (run numbers refer to conditions in Ref. 3).

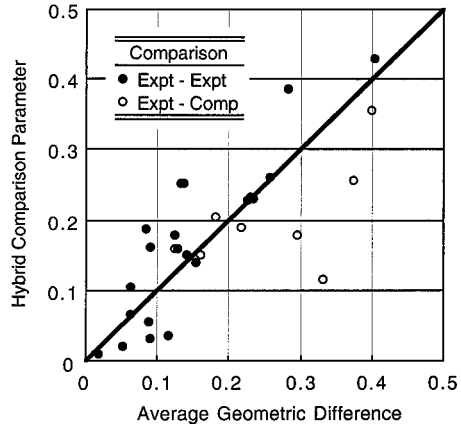

Fig. 10 Comparison parameters from hybrid and geometric comparison methods.

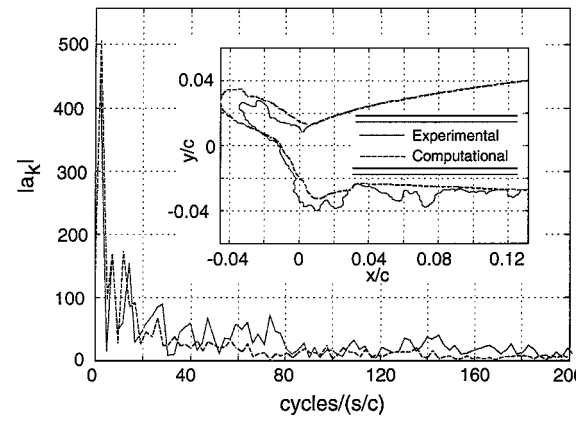

Fig. 11 Comparison of Fourier descriptor for an experimentally and computationally produced ice accretion (run number 204 from Ref. 3; hybrid comparison parameter equals 0.158).

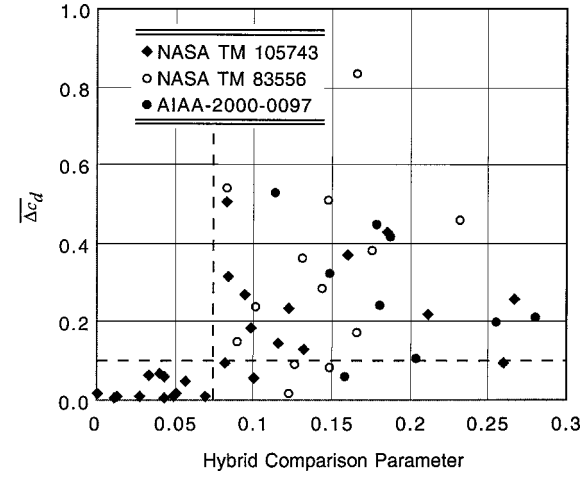

Fig. 12 Correlation of hybrid comparison parameter with normalized difference in drag coefficient.

for ice accretions formed at a range of icing conditions. Shin and Bond[26] measured the drag coefficient for 26 accretions and then predicted the shapes using an early version of LEWICE.[27] They[26] then calculated the drag coefficient for the computational shapes using an interactive boundary-layer method developed by Cebeci[28] and compared these values to the experimental values. As discussed earlier, Wright and Chung[3] recently calculated the aerodynamic performance parameters for 10 experimental ice accretions and the corresponding computational accretions produced by LEWICE for the same icing conditions. These ice shape data were digitized, and pairs of ice accretions were compared using the hybrid method. The fractional difference in the drag coefficient for each pair of accretions was also calculated using the equation

$$\overline{\Delta c_d} = \frac{2(c_{d,2} - c_{d,1})}{2(c_{d,2} + c_{d,1})} \tag{11}$$

The value of $\overline{\Delta c_d}$ was plotted as a function of the calculated comparison parameter as shown in Fig. 12. For values of the comparison parameter below approximately 0.075, the drag coefficients between the two ice accretions differ by less than 10%. For values above 0.075, the fractional difference in drag coefficient increases significantly and can be as great as 0.50 or more. As expected, as the values of the hybrid comparison parameter and, therefore, the geometric differences between the two ice accretions, increases, the drag coefficient varies considerably, depending on specifically how the ice accretions differed. Note that 14 of the ice shape comparisons from Shin and Bond[26] included in Fig. 12 are comparisons between experimentally produced and computationally produced

ice accretions. These data were found to be consistent with the other experiment-to-experiment comparisons shown in Fig. 12, and they demonstrate that this method can accurately quantify differences between experimental and computed ice accretions. The data of Wright and Chung,[3] indicated by the solid circles in Fig. 12, have values of the hybrid comparison parameter greater than 0.075 and, accordingly, larger differences between the normalized drag coefficients.

Wright and Chung[3] performed a regression analysis to determine which of the 11 ice shape parameters listed and defined in Ref. 3, as well as the Fourier error parameters defined by Eqs. (8) and (9), correlated best with the lift, drag, and moment coefficients. They found that these aerodynamic performance parameters were most sensitive to the upper horn angle, upper horn thickness, leading-edge minimum thickness, and the frequency-weighted difference in Fourier coefficients. For many accretions, the maximum forward width and maximum thickness used in the hybrid method locates the same point on the accretion used to calculate the horn angle and thickness used by Wright and Chung[3] (compare the definitions of these parameters shown in Figs. 1 and 7). Also, at angles of attack near 0 deg, the point used to measure the thickness at $y = 0$ used in the hybrid method is close to the point used to determine the leading-edge minimum thickness. Obviously, the selection of comparison parameters is not unique, and different parameters can provide different quantifications of the same feature on an ice accretion. Evaluating comparison methods then becomes a matter of how well they satisfy the requirements listed at the beginning of this paper.

Conclusions

The objective of this work was to develop an automated method to quantify the merit of a comparison of ice accretions. A practical method must not only provide quantitative information to compare ice accretions, but should satisfy as many of the following requirements as possible. The method should be 1) easy to apply at different icing facilities; 2) applicable to glaze, rime, and mixed icing conditions; 3) applicable to the comparison of experimentally and numerically produced ice accretions; 4) independent of test article geometry; and 5) free from the subjectivity of the operator.

Additionally, ice shapes that are found to compare well using such a method should have similar aerodynamic performance. A method that combines the automatic measurement and comparison of several local geometric features and metrics of the Fourier descriptors of the two ice accretion profiles was developed. The entire process was performed in the MATLAB programming environment to increase the consistency and objectivity of the analysis. The average difference parameter obtained from the hybrid comparison method yielded results that were consistent with comparisons made both visually and based on fractional differences of geometric characteristics. The use of the hybrid method eliminates problems associated with defining geometric characteristics that are applicable for experimentally or computationally produced ice accretions formed in glaze, rime, and mixed icing conditions. Furthermore, ice shapes for which the comparison parameter was less than 0.075 (7.5%) were found to have drag coefficients that differed by less than 10%. Other, more specific conclusions drawn from the results presented follow:

1) The P-Fourier transform method provides an excellent method of obtaining coordinates for smoothed simulated ice accretions used in certain types of icing tests. This is accomplished by calculating the Fourier descriptor for an ice accretion shape, setting all frequencies greater than some cutoff frequency to zero, and performing an inverse Fourier transform.

2) Glaze, rime, and mixed ice accretions can be differentiated by their Fourier descriptors. Horns on a glaze or mixed ice accretion produce Fourier descriptors having significant contributions at higher frequencies than those found in rime ice accretions. Computational ice accretions generally lack the higher frequency components because the mechanisms governing the formation of surface roughness are not modeled.

3) Frequencies less than 100 cycles/(s/c) are required to accurately represent an ice accretion shape and should be included in the calculation of difference terms from the P-Fourier descriptor.

4) The method developed in this work is applicable to the comparison of experimentally and computationally produced ice accretions.

With this method, the quantitative comparison of ice accretion profiles can be made more consistently and objectively. In addition to providing a method of comparing ice accretions formed at different ground-test facilities, this comparison method can help researchers quantify the improvement of an ice shape prediction resulting from modifications to the ice accretion model. It can also assist in the development and validation of icing scaling methods by providing a quantitative method of evaluating the relative performance of scaling methods. The global representation of the ice accretion using its P-Fourier transform is a unique analysis tool that may be able to quantify the small-scale surface roughness on ice accretions that is so critical in the heat transfer processes. Future work on the effect of surface roughness on heat transfer will investigate the usefulness of the procedure.

Acknowledgment

This work was supported by NASA John H. Glenn Research Center at Lewis Field through Grant NAG3-2171. The author also wishes to thank David N. Anderson for planning and conducting the icing scaling tests in the Icing Research Tunnel at NASA John H. Glenn Research Center at Lewis Field.

References

[1]Ruff, G. A., and Anderson, D. N., "Quantification of Ice Accretions for Icing Scaling Evaluations," AIAA Paper 98-0195, Jan. 1998.

[2]Wright, W. B., and Rutkowski, A., "Validation Report for LEWICE 2.0," NASA CR-1999-208690, Jan. 1999.

[3]Wright, W. B., and Chung, J., "Correlation Between Geometric Similarity of Ice Shapes and the Resulting Aerodynamic Performance Degradation—A Preliminary Investigation using WIND," NASA CR-1999-209417, Jan. 2000; also AIAA Paper 2000-0097, Jan. 2000.

[4]Cook, D. E., "Relationship of Ice Shapes and Drag to Icing Condition Dimensionless Parameters," AIAA Paper 2000-0486, Jan. 2000.

[5]Potapczuk, M. G., "A Review of NASA Lewis' Development Plans for Computational Simulation of Aircraft Icing," NASA TM-1999-208904, Jan. 1999; also AIAA Paper 99-0243, Jan. 1999.

[6]Wright, W. B., "Users Manual for the NASA Lewis Ice Accretion Code LEWICE 2.0," NASA CR-1999-209409, Sept. 1999.

[7]Gray, V. H., "Correlations Among Ice Measurements Impingement Rates, Icing Conditions and Drag Coefficients for an Unswept NACA 65A004 Airfoil" NACA TN-4151, Feb. 1958.

[8]Gray, V. H., "Prediction of Aerodynamic Penalties Caused by Ice Formations on Various Airfoils," NASA TN D-2166, Feb. 1964.

[9]Shaw, R. J., Sotos, R. G., and Salano, F. R., "Experimental Study of Airfoil Icing Characteristics," AIAA Paper 82-0283, Jan. 1982.

[10]Olsen, W., Shaw, R. J., and Newton, J., "Ice Shapes and the Resulting Drag Increase for a NACA 0012 Airfoil," NASA TM-83556, Jan. 1984.

[11]Papadakis, M., Alansatan, S., and Seltmann, M., "Experimental Study of Simulated Ice Shapes on a NACA 0011 Airfoil," AIAA Paper 99-0096, Jan. 1999.

[12]Lee, S., Kim, H. S., and Bragg, M. B., "Investigation of Factors that Influence Iced-Airfoil Aerodynamics," AIAA Paper 2000-0099, Jan. 2000.

[13]Cosgriff, R. L., "Identification of Shape," Ohio State Univ. Research Foundation, Rept. 820-11, ASTIA AD 254-792, Columbus, OH, Dec. 1960.

[14]Zahn, C. T., and Roskies, R. Z., "Fourier Descriptors for Plane Closed Curves," *IEEE Transactions on Computers*, Vol. C-21, No. 3, 1972, pp. 269–281.

[15]Uesaka, Y., "A New Fourier Descriptor Applicable to Open Curves," *Transactions of the IECE—Japan*, Vol. J67-A, No. 3, 1984, pp. 166–173.

[16]Aibara, T., and Ohue, K., "Human Face Profile Recognition by a P-Fourier Descriptor," *Optical Engineering*, Vol. 32, No. 4, 1993, pp. 861–863.

[17]Kushnir, M., Abe, K., and Matsumoto, K., "An Application of the Hough Transform to the Recognition of Printed Hebrew Character," *Pattern Recognition*, Vol. 16, No. 2, 1983, pp. 183–191.

[18]Huang, J. S., and Lung, M., "Separating Similar Complex Chinese Characters by Walsh Transform," *Pattern Recognition*, Vol. 20, No. 4, 1987, pp. 425–428.

[19]Sarvarayudu, G. P. R., and Sethi, I. K., "Walsh Descriptors for Polygonal Curves," *Pattern Recognition*, Vol. 16, No. 3, 1983, pp. 327–336.

[20]Chen, G. Y., and Bui, T. D., "Invariant Fourier-Wavelet Descriptor for

Pattern Recognition," *Pattern Recognition*, Vol. 32, No. 7, 1999, pp. 1083–1088.

[21]Govindan, V. K., and Shivaprasad, A. P., "Character Recognition—A Review," *Pattern Recognition*, Vol. 23, No. 7, 1990, pp. 671–683.

[22]Shridhar, M., and Badreldin, A., "High Accuracy Character Recognition Algorithm Using Fourier and Topological Descriptors," *Pattern Recognition*, Vol. 17, No. 5, 1984, pp. 515–524.

[23]Cheng, D. H., and Yan, H., "Recognition of Handwritten Digits Based on Contour Information," *Pattern Recognition*, Vol. 31, No. 2, 1998, pp. 235–255.

[24]Anderson, D. N., and Ruff, G. A., "Evaluation of Methods to Select Scale Velocity in Icing Scaling Tests," AIAA Paper 99-0244, Jan. 1999.

[25]"Using MATLAB," The MathWorks, Inc., Natick, MA, Jan. 1998.

[26]Shin, J., and Bond, T. H., "Experimental and Computational Ice Shapes and Resulting Drag Increase for a NACA 0012 Airfoil," NASA TM-105743, Jan. 1992.

[27]Ruff, G. A., and Berkowitz, B. M., "Users Manual for the NASA Lewis Ice Accretion Prediction Code (LEWICE)," NASA CR-185129, May 1990.

[28]Cebeci, T., "Calculation of Flow Over Iced Airfoils," *AIAA Journal*, Vol. 27, No. 7, 1989, pp. 853–861.